

STATISTICAL SIMULATION OF THE PROCESS OF ACOUSTIC RADIATION PROPAGATION THROUGH THE MOVING TURBULENT ATMOSPHERE WITH ALLOWANCE FOR REFRACTION

V. V. Belov,^{1,2} Yu. B. Burkatskaya,³ N. P. Krasnenko,^{4,5}
M. V. Tarasenkov,¹ and L. G. Shamanaeva¹

UDC 551.596

The Monte–Carlo method is used to solve the problem of sound propagation through the lower plane-stratified 500-meter layer of the moving turbulent atmosphere. Quantitative estimates of the intensity of transmitted and multiply scattered radiation are obtained with allowance for the influence of the refraction effects.

Keywords: sound propagation through the atmosphere, multiple scattering and refraction of sound, Monte–Carlo method.

INTRODUCTION

Difficulties of the analytical approach to a solution of the problem on sound propagation through the atmosphere necessitate the involvement of numerical methods. In [1–9], the method of statistical simulation (Monte–Carlo) was used by the authors to solve the problem of acoustic radiation propagation through the plane-stratified motionless turbulent atmosphere, and quantitative estimates of the contribution of multiply scattered radiation to the transmitted radiation intensity were obtained.

In the present work, the process of acoustic radiation propagation through the lower plane-stratified 500-meter layer of the moving turbulent atmosphere was simulated taking into account the refraction effects, and statistical estimates of the transmitted radiation intensity and contribution of multiply scattered radiation were obtained for sound frequencies in the range 1000–4000 Hz. The refraction of sound occurs on gradients of the atmospheric temperature and wind velocity and leads to wind shear of the sound wave and occurrence of additional attenuation due to the curvature of the trajectory of its propagation [10–11]. In the daytime, the temperature usually decreases with altitude, which causes the corresponding changes in the sound propagation velocity, and the trajectories of sound wave propagation are symmetrically bent up. When the wind velocity increases with altitude, the trajectories of sound ray propagation in the leeward direction are convex, and the trajectories of sound wave propagation in the windward direction are concave [12]. In [13] it was noted that the attenuation of sound propagating in the windward direction can differ significantly from that of sound propagating in the leeward direction, which testifies to the necessity of consideration of the refraction effects in the study of acoustic radiation propagation.

In the first section, the acoustic model of the plane-stratified moving atmosphere is described, and model vertical profiles of the wind velocity used in our calculations are presented together with the total acoustic radiation attenuation coefficient and the phonon survival probabilities for sound frequencies in the range 1000–4000 Hz. In the second section, the geometrical aspects of the examined problem and some special features of the modified

¹V. E. Zuev Institute of Atmospheric Optics of the Siberian Branch of the Russian Academy of Sciences, Tomsk, Russia; ²National Research Tomsk State University, Tomsk, Russia; ³National Research Tomsk Polytechnic University, Tomsk, Russia; ⁴Institute of Monitoring of Climatic and Ecological Systems of the Siberian Branch of the Russian Academy of Sciences, Tomsk, Russia; ⁵Tomsk State University of Control Systems and Radioelectronics, Tomsk, Russia, e-mail: belov@iao.ru; sima@iao.ru; krasnenko@imces.ru. Translated from *Izvestiya Vysshikh Uchebnykh Zavedenii, Fizika*, No. 11, pp. 100–107, November, 2011. Original article submitted June 15, 2011.

computational algorithm connected with allowance for the refraction are discussed. Results of Monte-Carlo calculations of the transmitted acoustic radiation intensity and contribution of multiply scattered radiation with the use of the modified computational algorithm are presented in section 3.

1. ACOUSTIC MODEL OF THE PLANE-STRATIFIED MOVING ATMOSPHERE

In this work, the problem of acoustic radiation propagation through the lower 500-meter layer of the plane-stratified moving turbulent atmosphere was solved. Calculations were performed for the acoustic model of the atmosphere based on the theoretical estimates of sound scattering by the atmospheric turbulence presented in [14] for the von Karman spectra of the atmospheric temperature and wind velocity fluctuations [15]. The atmosphere was subdivided into 25 layers 20 m each with the coefficients of classical and molecular absorption and scattering on turbulent temperature and wind velocity fluctuations that were considered constant within these layers. In calculations of the altitude dependence of the absorption and scattering coefficients, the vertical profiles of the pressure, sound speed, and atmospheric temperature were taken for the standard model of the middle-latitude summer atmosphere [16].

The vertical profile of the wind speed for the unstable atmospheric stratification was logarithmic:

$$V(z) = \frac{V_*}{\varepsilon} \ln \frac{z}{z_0}, \quad (1)$$

where $\varepsilon = 0.4$ is the von Karman constant, V_* is the friction velocity (the velocity scale in the near-ground layer), and z_0 is the parameter of underlying surface roughness. In our calculations, we used $z_0 = 2$ cm (grass cover). Calculations were performed for wind velocities at the wind vane altitude $z = 10$ m equal to 0, 2, 4, 6, 8, and 10 m/s. The wind was directed along the x axis.

The formulas for calculations of the classical (σ_{cl}) and molecular absorption coefficients (σ_{mol}) and coefficients of scattering on the atmospheric temperature (σ_T) and wind velocity fluctuations (σ_V) depending on the atmospheric temperature T , air humidity, sound frequency F , and outer scale of atmospheric turbulence L_0 as well as compact formulas for the normalized phase functions of sound scattering on atmospheric temperature, $g_T(\theta)$, and wind velocity fluctuations, $g_V(\theta)$, as functions of the scattering angle θ , were presented in [2]. The vertical profiles of the coefficients of total attenuation

$$\sigma_{att}(z_j) = \sigma_{cl}(z_j) + \sigma_{mol}(z_j) + \sigma_T(z_j) + \sigma_V(z_j) \quad (2)$$

and phonon survival probabilities

$$P_{sc}(z_j) = [\sigma_T(z_j) + \sigma_V(z_j)] / \sigma_{att}(z_j), j = 1 \dots, 25, \quad (3)$$

for sound frequencies in the range $F = 1000$ –4000 Hz and outer scale of turbulence $L_0 = 80$ m were presented in [9]. The corresponding vertical profiles for the outer scale $L_0 = 10$ m are shown in Fig. 1.

From Fig. 1a it can be seen that for frequency $F = 4000$ Hz and altitudes $z \leq 240$ m, σ_{att} depends strongly on the altitude, decreasing from 0.014 m^{-1} in the surface layer to 0.009 m^{-1} at $z = 240$ m; with further increase in altitude, it remains practically constant. For frequencies ≤ 3000 Hz, σ_{att} depends weakly on the altitude. The essential dependence of the total attenuation coefficient on the outer scale of turbulence should also be noted. Thus, whereas $\sigma_{att} = 0.21 \text{ m}^{-1}$ in the surface layer for $L_0 = 80$ m and $F = 4000$ Hz [9], as can be seen from Fig. 1a, $\sigma_{att} = 0.014 \text{ m}^{-1}$ for $L_0 = 10$ m and the same frequency, that is, it decreases by 93%. In addition, whereas the excess turbulent attenuation for $L_0 = 80$ m is comparable with the molecular absorption at a frequency of 2000 Hz ($P_{sc} \geq 0.5$) [9], as can be seen from Fig. 1, it remains smaller than the molecular absorption ($P_{sc} \geq 0.46$) for the entire range of sound frequencies and $L_0 = 10$ m.

Figure 2 shows the normalized phase functions of sound scattering on temperature and wind velocity fluctuations for the outer scale of turbulence $L_0 = 10$ m; the corresponding scattering phase functions for the outer scale $L_0 = 80$ m were presented in [9].

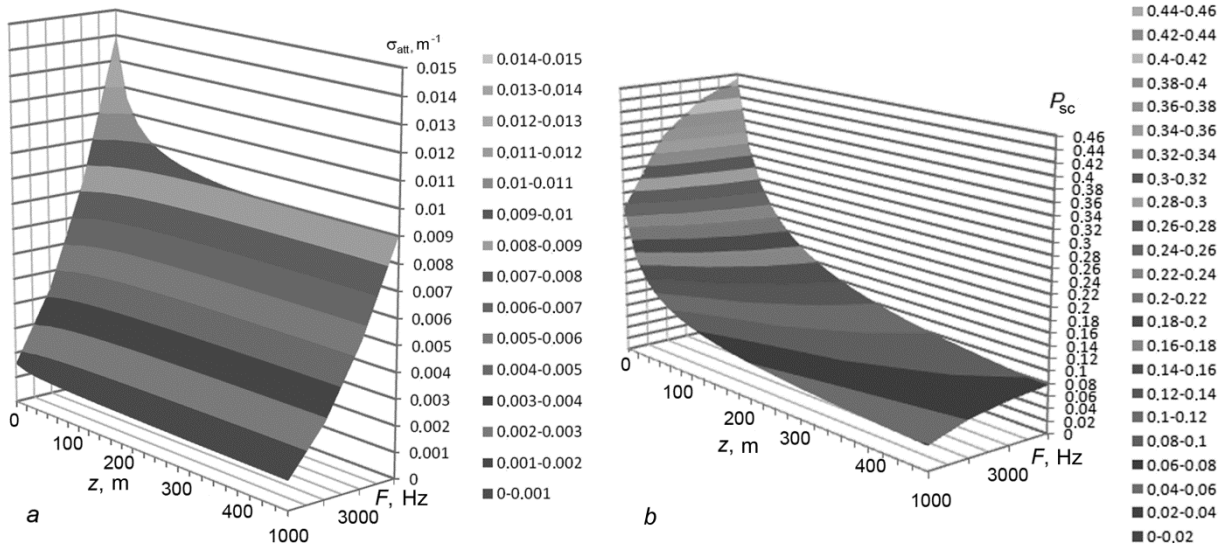


Fig. 1. Vertical profiles of the coefficient of total sound attenuation (a) and probabilities of phonon survival (b) for frequencies $F = 1000\text{--}4000$ Hz and outer scale of turbulence $L_0 = 10$ m.

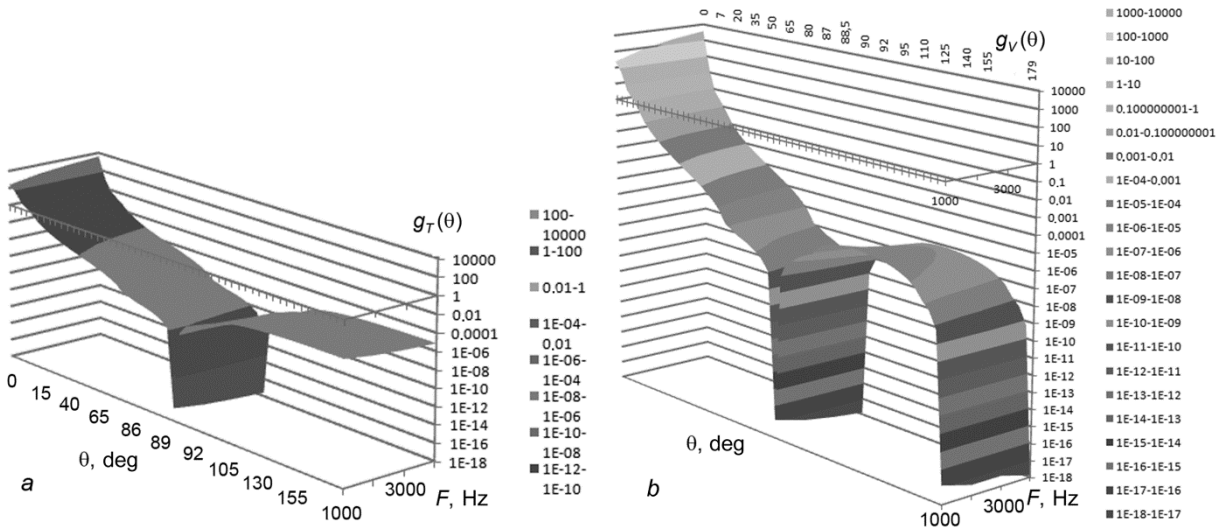


Fig. 2. Normalized phase functions of sound scattering on temperature (a) and wind velocity fluctuations (b) for frequencies $F = 1000\text{--}4000$ Hz and outer scale of turbulence $L_0 = 10$ m.

2. GEOMETRICAL ASPECTS OF THE PROBLEM AND SOME SPECIAL FEATURES OF THE MODIFIED COMPUTATIONAL ALGORITHM

The problem of vertical propagation of radiation of the source having acoustic power of 1 W with circular aperture 1 m in diameter, beam divergence angle $\phi = 2.5\text{--}25^\circ$, and distribution density

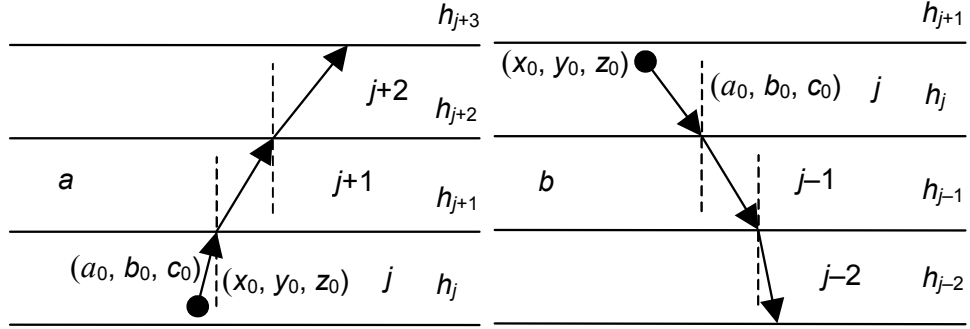


Fig. 3. Trajectories of phonon propagation through the medium.

$$f(R) = A \left(\cos^2 \left(\frac{\pi R_s}{2} \right) + 0.1 \right) \quad (4)$$

was solved, where $0 \leq R_s \leq 0.5$ and constant A was chosen from the normalization condition. The distribution density of the initial directional cosine of the angle with the Oz axis was a Gaussian one. The radiation source was localized on the Oz axis at the altitude $H_s = 35$ m above the absolutely absorbing Earth's surface. Taking into account the symmetry of the problem, the dependence of the transmitted and multiply scattered radiation intensity over the horizontal plane of the detector was estimated as a function of the distance H from the vertical axis counted in the positive (windward) and negative (leeward) directions of the x axis.

The computational algorithm whose flow chart was presented in [7] was modified to solve the problem of acoustic radiation propagation through the plane-stratified moving atmosphere with allowance for the refraction effects. The procedure *Geom_r* was used that allowed distances to the boundaries of the layers into which the plane-parallel atmosphere was subdivided and directions of rays in each layer to be calculated.

The input data for the procedure are the serial number of the current layer j , initial phonon coordinates $\mathbf{r}_0 = (x_0, y_0, z_0)$, and initial direction of phonon emission $\omega_0 = (a_0, b_0, c_0)$. The geometrical schemes of the trajectories of phonon propagation in the positive direction of the z axis (toward the upper boundary of the atmosphere, $c_1 > 0$) and on the contrary, in the direction toward the underlying surface ($c_1 < 0$) are shown in Fig. 3a and b, respectively.

Let $\mathbf{R}(x, y)$ be the horizontal phonon coordinates; then according to [17],

$$\frac{\partial \mathbf{R}}{\partial z} = \frac{C \kappa \cos \xi + \frac{[C(w_0 - V_h \kappa \cos \xi) - V_z \chi] V_h}{(C^2 - V_z^2)}}{\chi}, \quad (5)$$

where C is the current sound speed, $\kappa = i \cos v + j \sin v$, v is the azimuth of the normal \mathbf{n} at the point of phonon emission, ξ is the angle between \mathbf{n} and the horizontal plane (the angle of normal sliding) at the point of phonon emission,

$$w_0 = C_0 + V_{h0} \kappa \cos \xi + V_{z0} \sin \xi \quad (6)$$

is the phase velocity of sound at the point of phonon emission, C_0 , V_{h0} , and V_{z0} are values of the sound speed and horizontal and vertical components of the wind velocity at the point of phonon emission,

$$\chi = \pm \sqrt{(w_0 - V_h \kappa \cos \xi)^2 - (C^2 - V_z^2) \cos^2 \xi} \quad (7)$$

is the parameter with the “+” sign for the ascending ray and the “–” sign for the descending ray. At the point of ray rotation, we have $\chi = 0$. In numerical calculations, it was determined by the iterative method from the condition $\chi = 0$, and the phonon trajectories before and after this point were then calculated separately.

In our model, $V_z = V_{z0} = 0$, and vectors V_{h0} and V_h were directed along the Ox axis. The atmosphere was plane-stratified, and the layers were parallel to the Earth’s surface. Taking this into account, the calculation formulas assume the form

$$\frac{\Delta x}{\Delta z} = \frac{C \cos v \cos \xi + \frac{w_0 V_h}{C}}{\chi}, \quad \frac{\Delta y}{\Delta z} = \frac{C \sin v \cos \xi}{\chi}, \quad (8)$$

$$w_0 = C_0 + V_{h0} \cos v \cos \xi, \quad \chi = \pm \sqrt{(w_0 - V_h \cos v \cos \xi)^2 - C^2 \cos^2 \xi}. \quad (9)$$

In the procedure, the following quantities were calculated:

- 1) the number of layers n_l intersected by the phonon trajectory up to the atmospheric boundary;
- 2) distances l_i from the point $r_0 = (x_0, y_0, z_0)$ to the boundaries of layers of the plane-parallel atmosphere along the trajectory (which is a broken line), $i = 1, \dots, n_l$;
- 3) acoustic thickness τ along the trajectory from the point $r_0 = (x_0, y_0, z_0)$ to the boundary of the atmosphere along the ray;
- 4) coordinates (x_i, y_i, z_i) of points of ray intersections with the layer boundaries, $i = 1, \dots, n_l$;
- 5) directional cosines (a_i, b_i, c_i) of the phonon in each layer.

The algorithm of calculations of the above-indicated quantities is the following.

1. The phonon free path τ is modeled using the formula $\tau = -\ln(\text{rand})$, where rand is a random variable uniformly distributed in the interval $[0, 1]$. We set $i = 1$ and $j_0 = j$.
2. Distances from the point r_0 to the layer boundaries are calculated. The calculation formulas, depending on the direction of phonon propagation, have the form
– for $c_1 < 0$:

$$l_0 = 0, \quad l_1 = (h_j - z_0) / c_1, \quad (10)$$

– for $c_1 > 0$:

$$l_0 = 0, \quad l_1 = (h_{j+1} - z_0) / c_1. \quad (11)$$

3. The acoustic path length of the trajectory from the point $r_0 = (x_0, y_0, z_0)$ to the boundary of the subsequent layer of the atmosphere is calculated:

$$L = l_1 \sigma_{\text{att}}(j). \quad (12)$$

If $L > \tau$, we set

$$L = \tau \quad l_1 = L / \sigma_{\text{att}}(j). \quad (13)$$

4. The coordinates of the next point of the trajectory change are calculated:

$$x_1 = x_0 + a_0 l_1, \quad y_1 = y_0 + b_0 l_1, \quad z_1 = z_0 + c_0 l_1. \quad (14)$$

5. If $L < \tau$, the ray direction in the subsequent layer of the atmosphere is calculated:

$$w_0 = C(j_{i-1}) + V(j_{i-1})a_{i-1}, \quad \chi = \text{sign}(c_{i-1})\sqrt{(w_0 - V(j_i)a_{i-1})^2 - \left(C(j_i)\sqrt{1-c_{i-1}^2}\right)^2}. \quad (15)$$

Otherwise, go to item 10.

6. The coordinates of the intersection point of the trajectory with the boundary of the subsequent layer are calculated:

$$\Delta x = \left(\frac{(w_0 - V(j_i)a_{i-1})V(j_i)}{C(j_i)} + C(j_i)a_{i-1} \right) \frac{\text{sign}(c_{i-1})\Delta h}{\chi}, \quad \Delta y = C(j_i)b_{i-1} \frac{\text{sign}(c_{i-1})\Delta h}{\chi}, \quad \Delta z = \Delta h. \quad (16)$$

We set $i = i + 1$,

$$x_i = x_{i-1} + \Delta x, \quad y_i = y_{i-1} + \Delta y, \quad z_i = z_{i-1} + \Delta z. \quad (17)$$

7. The acoustic path length of the phonon in the subsequent layer is calculated:

$$S_i = \sqrt{(\Delta x)^2 + (\Delta y)^2 + (\Delta z)^2}, \quad (18)$$

$$l_i = \sigma_{\text{att}}(i)S_i. \quad (19)$$

8. The directional cosines are calculated from the formulas

$$a_i = \frac{\Delta x}{S_i}, \quad b_i = \frac{\Delta y}{S_i}, \quad c_i = \text{sign}(c_{i-1})\frac{\Delta z}{S_i}. \quad (20)$$

9. If $L + l_i < \tau$, we set $L = L + l_i$ and go to item 5. Otherwise, we set $S_i = (\tau - L)/\sigma_{\text{att}}(i)$ and recalculate the coordinates of the point of the subsequent event:

$$x_i = x_{i-1} + a_i S_i, \quad y_i = y_{i-1} + b_i S_i, \quad z_i = z_{i-1} + c_i S_i. \quad (21)$$

10. End of the procedure. New event (absorption or scattering) is modeled.

Calculations were performed on a personal computer for 10^7 phonon histories, which provided the error in the region of the intensity maximum in the range 3–10%. The time of calculation of an individual realization did not exceed 10–15 min. Results of calculations are presented below.

3. STATISTICAL ESTIMATES OF THE INFLUENCE OF THE REFRACTION ON THE DISTRIBUTION OF THE TRANSMITTED ACOUSTIC RADIATION INTENSITY

Figure 4 shows the distribution of the transmitted, I_{tr} (a and c), and multiply scattered radiation intensities, I_{ms} (b and d) for the source having acoustic power of 1 W, circular aperture 1 m in diameter, and Gaussian distribution as a function of the distance H from the Oz axis in the windward ($H > 0$) and leeward ($H < 0$) directions for sound frequencies $F = 1000$ Hz (a and b) and 4000 Hz (c and d), source divergence angle $\phi = 2.5^\circ$, and wind velocities at the altitude $z = 10$ m indicated in the figure. The corresponding distributions of the radiation intensity calculated without refraction are also shown in the figure.

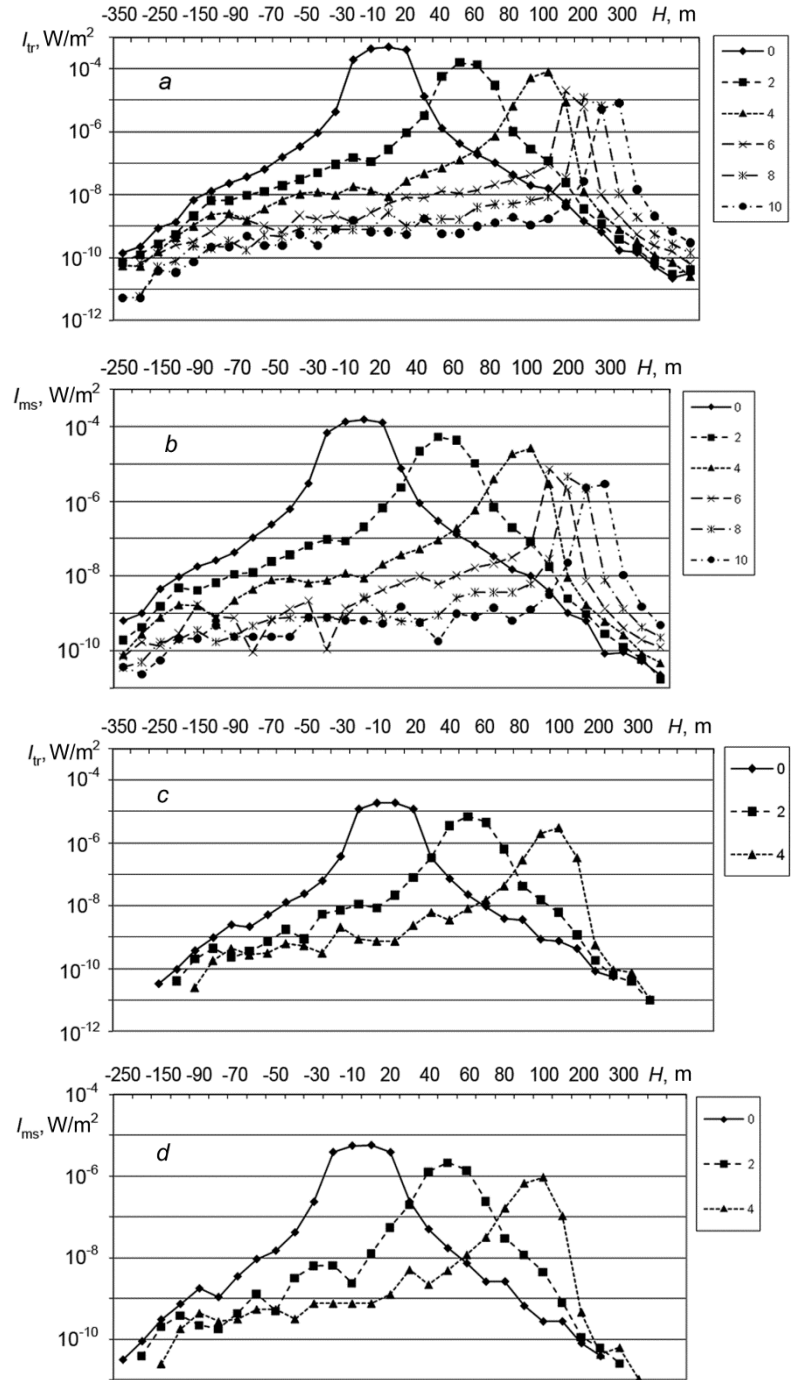


Fig. 4. Distribution of the transmitted (I_{tr} , *a* and *c*) and multiply scattered acoustic radiation intensities (I_{ms} , *b* and *d*) over the detector zones with allowance for the refraction as functions of the distance H from the Oz axis for $F = 1000$ Hz (*a* and *b*) and 4000 Hz (*c* and *d*), $L_0 = 80$ m (*a* and *b*) and 15 m (*c* and *d*), source divergence angle $\phi = 2.5^\circ$, and wind velocities at the weather vane altitude $z = 10$ m, in m/s, indicated at the upper right of the figure.

From Fig. 4 it can be seen that the shift of the maxima of the transmitted and multiply scattered radiation intensities in the wind direction is proportional to the wind speed. Without refraction, the maximum of the transmitted

radiation intensity at a frequency of 1000 Hz is $I_{\text{tr max}} = 5.03 \cdot 10^{-4} \text{ W/m}^2$, and with allowance for the refraction, $I_{\text{tr max}} = 1.62 \cdot 10^{-4} \text{ W/m}^2$ for the horizontal wind speed at the weather vane altitude $V_{10} = 2 \text{ m/s}$, that is, it decreases 3 times. The contribution of multiple scattering to the transmitted radiation intensity in the region of maximum is 32%. The width of the distribution also decreases, and the distribution itself becomes more asymmetric with increasing vertical gradient of the wind speed.

From Fig. 4, c and d it can be seen that for a frequency of 4000 Hz without refraction, $I_{\text{tr max}} = 1.9 \cdot 10^{-5} \text{ W/m}^2$; at $V_{10} = 2 \text{ m/s}$, $I_{\text{tr max}} = 7 \cdot 10^{-6} \text{ W/m}^2$, that is, it decreases by a factor of 2.7.

CONCLUSIONS

In this work, the problem of acoustic radiation propagation through the moving turbulent atmosphere with allowance for the refraction effects has been solved by the Monte-Carlo method using the algorithm that takes into account the refraction effects. Quantitative estimates of the influence of the refraction effects and multiple scattering on sound propagation through the lower plane-stratified 500-meter layer of the atmosphere were obtained. It was established that for the considered geometry of the numerical experiment, the refraction causes the displacement of the transmitted radiation maximum along the wind direction proportional to the wind speed gradient; moreover, the width of the maximum decreases with increasing wind speed, and the additional radiation attenuation can reach a factor of 2.7–3. The contribution of multiple scattering to the transmitted radiation intensity in the region of maximum exceeded 30%.

REFERENCES

1. R. A. Baykalova, G. M. Krekov, and L. G. Shamanaeva, Opt. Atm. Okeana, **1**, No. 5, 25–30 (1988).
2. L. G. Shamanaeva and Yu. B. Burkatskaya, Russ. Phys. J., No. 12, 1296–1306 (2004).
3. L. G. Shamanaeva and Yu. B. Burkatskaya, in: Proc. 12th Int. Symp. on Acoustic Remote Sensing and Associated Techniques of the Atmosphere and Oceans, P. Anderson, S. Bradley, and S. von Hunerbein, eds., Cambridge, UK (2004), pp. 145–148.
4. L. Shamanaeva and Yu. Burkatskaya, in: Extended Abstracts of Reports Presented at the Int. Symp. for the Advancement of Boundary Layer Remote Sensing, S. Emeis, ed., Garmisch-Partenkirchen, Germany (2006), pp. 14–16.
5. L. G. Shamanaeva and Yu. B. Burkatskaya, Russ. Phys. J., No. 10, 1056–1060 (2007).
6. V. V. Belov, Yu. B. Burkatskaya, N. P. Krasnenko, and L. G. Shamanaeva, Russ. Phys. J., No. 12, 14–19 (2009).
7. V. V. Belov, Yu. B. Burkatskaya, N. P. Krasnenko, and L. G. Shamanaeva, in: Materials of XVI Int. Symp. “Atmospheric and Ocean Optics. Atmospheric Physics,” Tomsk (2009), pp. 142–146.
8. V. V. Belov, Yu. B. Burkatskaya, N. P. Krasnenko, and L. G. Shamanaeva, in: Extended Abstracts of Reports Presented at the 15th International Symposium for the Advancement of Boundary Layer Remote Sensing, Paris, France (2010). <http://www.isars2010.uvsq.fr>, P. P-RET/01-1-P-RET/01-4.
9. V. V. Belov, Yu. B. Burkatskaya, N. P. Krasnenko, and L. G. Shamanaeva, Opt. Atm. Okeana, **24**, No. 12, 1072–1077 (2011).
10. K. Attenborough, K. M. Li, and K. Horoshenkov, Predicting Outdoor Sound, Taylor & Francis, London; New York (2007).
11. E. M. Salomons, Computational Atmospheric Acoustics, Kluwer Academic Publishers, Dordrecht; Boston; London (2001).
12. V. E. Ostashev, Propagation of Sound in Moving Media [in Russian], Nauka, Moscow (1992).
13. M. E. Delany, Acustica, **38**, 201–223 (1977).

14. R. A. Baikalova, G. M. Krekov, and L. G. Shamanaeva, *J. Acoust. Soc. Amer.*, **83**, No. 4, 1332–1335 (1988).
15. A. S. Gurvich, A. I. Kon, V. L. Mironov, and S. S. Khmelevtsov, *Laser Radiation in the Turbulent Atmosphere* [in Russian], Nauka, Moscow (1976).
16. Yu. A. Glagolev, *Handbook of the Physical Parameters of the Atmosphere* [in Russian], Gidrometeoizdat, Leningrad (1970).
17. A. Ya. Bogushevich and N. P. Krasnenko, *Opt. Atm. Okeana*, **7**, No. 9, 1258–1274 (1994).